RSC Advances

ROYAL SOCIETY OF CHEMISTRY

www.rsc.org/advances

Journal Name

RSCPublishing

ARTICLE

Sulphur bridged [22]annulene[2.1.2.1]s based organic field-effect transistors: Interplay of the steric bulk and charge transport†

Cite this: DOI: 10.1039/x0xx00000x

Received 00th January 2012,
Accepted 00th January 2012

DOI: 10.1039/x0xx00000x

www.rsc.org/

Tarunpreet Singh Virk,[a] Kamaljit Singh,*[a] Yunke Qin,[b] Wei Xu,[b] and Daoben Zhu*[b]

New, neutral, slightly puckered aromatic *meso*-substituted tetrathia[22]porphyrin[2.1.2.1] (TTP) macrocyclic architectures display structure dependent p-type semiconductor behaviour and constitute molecular field effect transistors with high on/off ratio (1×10^6) and high mobility (0.32 $cm^2\ V^{-1}\ s^{-1}$) in thin films deposited on octadecyltrichlorosilane (OTS) modified SiO_2. In order to study the influence of steric bulk, molecules with an increasing steric bulk at the *meso*-position have been synthesized and studied both experimentally and theoretically. The charge transport behavior was evaluated from their thin film Organic field-effect transistor (OFET) devices. Single crystal analysis and thin film morphologies of the molecules showed that upon incorporating a branched hydrocarbon group at the *meso*-phenyl substituents of TTP not only alters face to face stacking pattern but also changes the morphology of the thin films from highly crystalline to amorphous, as well as lowers the solubility in organic solvents. Such features lead to deterioration of the performance of the organic semiconductors (OSCs) devices.

Introduction

The performance of organic field-effect transistors (OFET) depends upon key properties of the semiconductor component such as air stability, solubility, energy gap, film morphology etc., which are essentially tunable by structural modifications. Polymeric and microcrystalline oligoacenes,[1,2] oligofurans/thiophenes,[3] oligotriarylamines[4] etc. display efficient semiconductor performance in optoelectronics. However, understanding of structure-property relationship of new systems remains ever important aspect for further improvement. We recently introduced sulphur[5] and oxygen[6] bridged [22]annulene(2.1.2.1)s **1** and **2** respectively as efficient OFETs (Fig. 1). Among these 5,16-di-*p*-tolyl tetrathia[22]porphyrin(2.1.2.1) (**1**, R = *p*-tolyl) depicted high (0.63 $cm^2V^{-1}s^{-1}$) hole mobility in thin films.[5] The furan analogue, 5,16-diphenyl tetraoxa[22]porphyrin(2.1.2.1) **2** (R = Ph) was more stable and showed hole mobility of 0.29 $cm^2V^{-1}s^{-1}$.[6] We attributed this to the extended conjugation of these cyclic conjugated molecules, which lowers the reorganization energy and enhances intermolecular π-π overlapping. These values were among the highest of thin film OFETs and superior to the α-oligofurans (μ: 0.05 $cm^2V^{-1}s^{-1}$) and α-oligothiophenes (0.09 $cm^2V^{-1}s^{-1}$).[3]

Compared to polymers, **1**,**2** form good quality crystals and co-crystals with various acceptor molecules under ambient conditions. With 7,7',8,8'-tetracyanoquinodimethane (TCNQ),

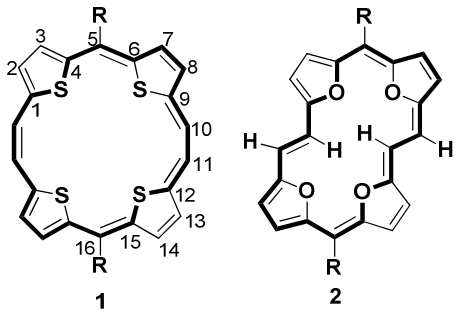

Fig. 1 Neutral sulphur and oxygen bridged [22]annulenes.

[a] *Department of Chemistry, Centre for Advanced Studies-I, Guru Nanak Dev University, Amritsar – 143 005, Punjab, India, Fax number: +91 183 2258819/20, E-mail: kamaljit19in@yahoo.co.in*

[b] *Beijing National Laboratory for Molecular Science, CAS Key Laboratory of Organic Solids, Institute of Chemistry, Chinese Academy of Sciences, Beijing – 100190, P. R. China. E-mail: wxu@iccas.ac.cn*

† Electronic Supplementary Information (ESI) available: Copies of ^1H, ^{13}C NMR, Mass, IR Spectra and full characterization, theoretical calculations details, figures and graphs, UV-Vis. spectra of thin films, TGA graphs, UV-Vis. and CV of **6b**,**c**, X-ray single crystal structure details with CCDC nos. 948111 and 986822, transfer and output curves. For ESI and crystallographic data in CIF or other electronic format see DOI: 10.1039/b000000x/

1 (R= Ph) formed self-assembled donor-acceptor π-π complex, described by us as "molecular level heterojunction" and depicted ambipolar charge transport behaviour (μ_h: 0.04, μ_e: 0.03 $cm^2V^{-1}s^{-1}$) in devices based on microcrystals in ambient conditions and showed great potential for use in light-emitting transistors, low cost devices and CMOS-like circuits.[7] Similar self-assembled fullerene/**1**(R = Ph) cocrystals forms a 2D segregated alternating layer structure with π-π interactions in both donor and acceptor layers, which, separately serve as paths for holes and electrons.[8] Organic single crystal field-effect transistors (OSCFETs) based on a series of tetrathia[22]porphyrin(2.1.2.1) [TTP] were also fabricated, combined with the device characterization and crystallographic analysis.[9]

Intrigued by their performance, we got interested in evaluating the effect of structural diversity at the *meso*- (5- and 16-) positions in order to draw a structure-property relationships. We now report on the synthesis and OFET characteristics of new TTPs appended with systematic increasing steric bulk at the key 5- and 16-positions. The hole-mobility and *on/off* ratios of these heteroannulenes has been correlated with the stacking patterns of TTPs as deduced from their single crystal structures as well as the change in their crystalline nature to amorphous nature upon attaching a bulky branched substituent.

Results and discussion

Using the dilithiation–formylation sequence (Scheme 1), di(thien-2-yl)methanes **3a-c** obtained through the condensation of the appropriate aldehyde with thiophene, could be conveniently di-formylated. Reductive McMurry coupling of the dialdehydes **4a–c** gave the corresponding 5,16-dihydrotetrathia[20]porphyrin(2.1.2.1) derivatives **5a–c** in high yield. The dehydrogenation of **5a–c** by DDQ occurred in toluene to give insoluble black complexes which were reduced by hydrazine to crystalline 5,16-disubstituted TTP derivatives **6a–c**. All compounds depicted satisfactory characteristic data (Page S3 to S49, ESI†).

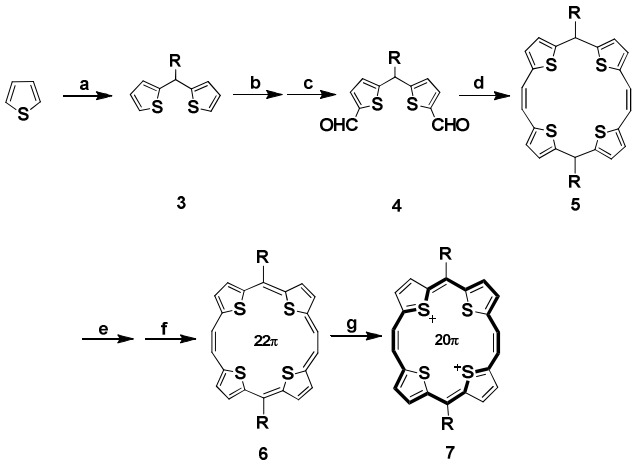

a, R = *p*-Et-C_6H_4; **b**, R = *p*-^{i}Pr-C_6H_4; **c**, R = *p*-^{t}Bu-C_6H_4

Scheme 1 (a) RCHO (0.33 mmol), Amberlyst 15, 80 °C; (b) *n*-BuLi (2.24 mmol), Et_2O, r.t.; (C) DMF (2.2 mmol), Et_2O; (d) Zn (21 mmol) / $TiCl_4$ (11 mmol), Pyridine (20 mmol), THF, reflux; (e) DDQ (3 mmol), toluene, r.t.; (f) Hydrazine, reflux; (g) conc. H_2SO_4.

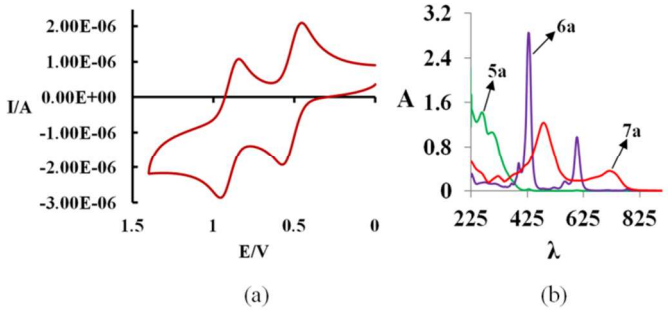

Fig. 2 (a) CV of **6a**; (b) UV-visible absorption spectra of **5a** (DCM), **6a** (DCM) and **7a** (H_2SO_4).

TGA indicated excellent thermal stability (Fig. S70 to S72, ESI†), with sublimation occurring prior to decomposition (>371 °C, **6a**; >391 °C, **6b** and >407 °C, **6c**). Further, the molecules showed exceptional air stability and did not require any inert atmosphere for handling/storing.

Like porphyrinoids, the aromatic **6a–c** adopt a near planar aromatic conformation and are, characterized by tendency to lose two electrons to form dicationic antiaromatic species **7** in solution as ascertained by the optical and electrochemical studies. π-Delocalization over the whole cyclic conjugated rings as well as aromaticity was revealed by the HOMOs and LUMOs of **6a-c**. The sulphur atoms showed greater contribution to HOMOs compared to LUMOs (Fig. S60 to S62, ESI†). Cyclic voltammogram (CV) of **6a** (Fig. 2a) in CH_2Cl_2 showed two reversible oxidation peaks at E^0_{ox} = 575 and 958 mV *vs.* SCE (calibrated using Fc/Fc^+ = 0.40 V *vs* SCE) indicating the formation of 20π dicationic species. The compounds **6b** and **6c** showed oxidation peaks at E^0_{ox} = 566 and 949 mV; 534 and 961 mV *vs.* SCE, respectively (Fig. S68 to S69, ESI†). Due to electron donating *p*-alkyl substituents, the oxidation potential values are lower than the TTPs **1** (R= *m*-Cl-C_6H_4 and *p*-F-C_6H_4) bearing electron withdrawing Cl or F substituents on the phenyl rings at 5- and 16-positions[10] and, consequently, facilitate the observed hole transportation. The CV data corresponds to HOMO energies of -4.83 eV (-4.4 - E^0_{ox} *vs* SCE), -4.86 eV and -4.82 eV, respectively for **6a-c** which are comparable to the work function of Au (-4.90 eV) suggesting an effective hole injection between electrode and semiconductor leading to improved performance. Due to low lying HOMO's, **6a-c** are highly stable as revealed from their TGA spectra.

The UV-visible (DCM) absorption spectra, showed a sharp and strong absorption maxima for **6a** at 429 nm (ε/$dm^3mol^{-1}cm^{-1}$ 284 500), compared to **5a** (Fig. 2b), and several weaker absorptions at wavelengths [394, 481, 516, 553, 601, 714 and 778 nm (ε/$dm^3mol^{-1}cm^{-1}$ 49 400, 3800, 5300, 27 200, 98 200, 1000 and 2700, respectively)]. The unsplit Soret band at 429 nm of the **6a** is analogous to the split Soret band at 415 and 433 nm of the low (C_2) symmetric **2** while the Q-type bands, appeared slight red shifted than porphycenes.[11] The band gaps of **6a-c** were estimated to be 1.57 eV from the absorption onsets. In analogy with systems **2**,[6] the 22π molecules **6a-c** were found to dissolve in sulfuric acid to give intense reddish-orange solution, indicative of formation of the dications **7a-c**, respectively (accompanied by the disappearance of sharp Soret bands and appearance of broadened absorption bands) (Fig. 2b and Fig. S63 to S64, ESI†). The UV-visible absorption data of

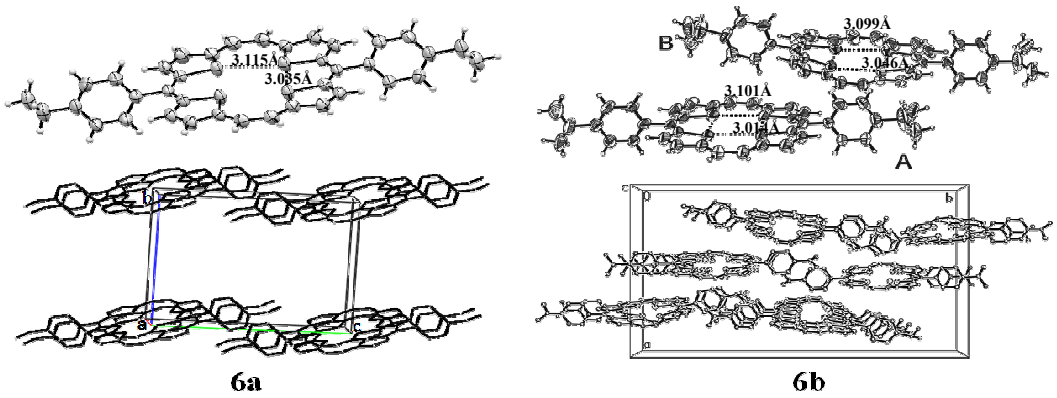

Fig. 3 X-ray crystal structures and stacking patterns of **6a** and **6b** viewed along a- and c-axes, respectively (H-atoms were omitted for clarity).

thin films (Fig. S65 to S67, ESI†) showed good correlation with the solution absorption spectra.

As a quantitative probe of aromaticity, we calculated Nucleus-Independent Chemical Shift, NICS(1) values using *ab initio* quantum mechanical DFT calculations at the B3LYP/6-311G(d) level using the Gauge Independent Atomic Orbitals (GIAO) method.[12] The shapes of the plots of the chemical shifts as a function of distance of the NICS probe (bq) from the molecular plane gave a clear indication of occurrence of diamagnetic ring currents (Fig. S49, S52, S55, ESI†). The large negative NICS(1) values of **6a** (-13.24 ppm), **6b** (-13.11 ppm) and **6c** (-13.36 ppm) at centre of molecules indicate a marginally greater degree of aromaticity compared to the oxygen bridged **2** (*ca* -13.17 ppm),[6] reflecting the enhanced ring currents in these systems. Positive NICS(1) (Fig. S58, ESI†) of dication **7b** (+7.3 ppm) on the other hand confirms its antiaromatic character. The aromaticity was further evidenced by its ^{1}H NMR and UV-visible absorption spectra. In ^{1}H NMR (Fig. S37, ESI†) of **6a**, a singlet at 11.03 ppm, corresponds to protons on the ethene carbons and an AB system corresponding to thiophene protons at 10.35 and 10.01 ppm. The aromatic protons appeared at 8.36 (4H) and 7.81 (4H) ppm. In contrast, no protons of the dihydro compound **5a** appeared downfield to 7.3 ppm. The solubility decreased markedly from **6a** to **6c**, bearing *p*-C_2H_5-C_6H_4, *p*-^{i}Pr-C_6H_4, and *p*-*tert*-butyl-C_6H_4 substituents at the *meso* positions thus providing us the guidelines to synthesize the solution processible organic materials.

Crystals of **6a** were obtained through slow evaporation of its toluene solution (For **6b**, methylene dichloride with a layer of toluene was used). **6a** crystallized in monoclinic unit cell and belongs to P 21/n space group (Table S5, ESI†) with unit cell parameters a = 8.3972 Å, b = 15.4871 Å, c = 11.8460 Å, $\alpha = \gamma = 90^o$, β = 92.993^o. The compound **6b** crystallized in orthorhombic unit cell and belongs to Pna 21 space group (Table S7, ESI†) with unit cell parameters a = 19.7591 Å, b = 34.5783 Å, c = 9.5257 Å, $\alpha = \beta = \gamma = 90^o$. Unlike, **1** (R = Ph),[5] the four sulfur atoms of **6a**,**b** are not in the same plane, as are the thiophene rings, similar to the sulphur bridged 18π annulene analogue ((18)annulene trisulfide)[13] in which the three thiophene units are totally out of the plane. In **6a**, two sulphur atoms linked through the *meso*-bridge are below the plane of the twisted macrocyclic ring, while the other set is well above. Out of the four sulfur atoms, the ones intercepted by four-carbon atoms are 3.115Å apart, while the neighboring sulfur atoms separated by a three-carbon bridge are 3.035Å apart. These distances are marginally shorter than twice the van der Waals radius of sulfur (3.60Å). The distances between the two sets of the opposite sulphur atoms are 4.344 and 4.355 Å. Further, we have found that the annulenes hosting bulkier *meso* groups are prone to slight ring puckering but maintain aromaticity. **6a** stacks into columns along the a-axis, in which the molecules adopt a face-to-face packing style (Fig. 3) which provides more efficient π-orbital overlap and facilitate charge transport. The intermolecular π–π interactions could be observed as the interplanar distance between the adjacent molecules in one stack is in the range of 3.4Å - 3.8Å. Such π–π overlapping provides the path for electron transport. The individual molecules are somewhat curved rather than fully planar, but show perfect transistor behavior.

Unlike the other TTPs, in the crystal structure of **6b**, the asymmetric unit contains two molecules (A and B) which stack into columns along the c-axis (Fig. 3). The molecules adopt a shifted face to face stacking pattern with the intermolecular distance slightly smaller than sum of the van der Waal radius of two carbon atoms, showing π-π interactions. In both A and B, the set of sulfur atoms intercepted by four carbon bridge points below the mean plane of the macrocycle while the other set points up. This distortion is reflected by slight variation between the otherwise identical adjacent and diagonal distances between the sulphur atoms of the macrocyles. Thus, in unit A, the two sulphur atoms intercepted by four-carbon bridge are 3.101 and 3.125 Å apart, while those intercepted by a three-carbon bridge are 3.030 and 3.014 Å apart. In B, the two sulfur atoms intercepted by the four-carbon bridge are 3.099 and 3.098 Å apart, while those separated by a three-carbon bridge are 3.036 and 3.046 Å apart. These distances are marginally shorter than twice the van der Waals radius of sulfur (3.60 Å). Four short contacts were present between the two molecules. The diagonal distance between the two sets of sulphur atoms in A are 4.354 and 4.320 Å, while these are 4.375 and 4.308 Å in B. As no significant π-π interactions could be observed between adjacent columns, **6b** was expected to possess quasi-one dimensional electrical transport properties.

Like aromatic porphyrinoids, **6a**,**b** are purple crystalline compounds but not as planar as the TTP **1** (R = Ph). This is also indicated by the torsion angles between all sulphur atoms (Table S6, S8, ESI†). Electron delocalization was expected and

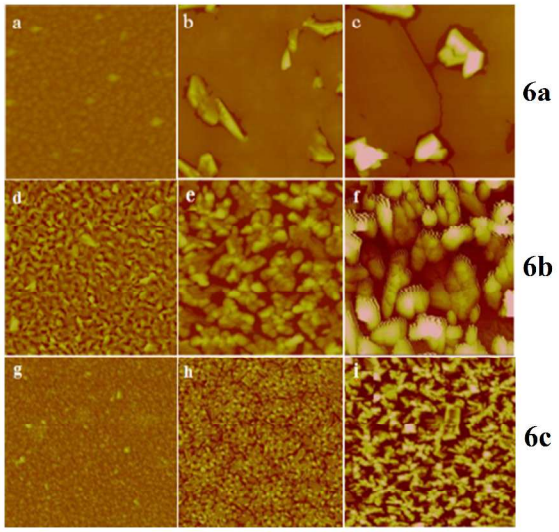

Fig. 4 AFM images (5 μm × 5 μm) of 50 nm thick films: **6a-c**, (a,d,g) T_s = 25 °C; (b,e,h) T_s = 60 °C; (c,f,i) T_s = 100 °C. Here T_s is the substrate temperature during film deposition.

is attested by the carbon–carbon distances in the thiophene rings as well as the macrocycle. The thiophene units show the bond length relation Cα–Cβ>Cβ–Cβ in agreement with electron delocalized porphyrinoids. The centrosymmetric tetrathiaporphyrin dication with four thiophene rings tilted up and down from the mean plane by 22.8° and 3.7°, respectively, also showed the above bond length relationship.[11]

Morphologies of the thin (50 nm) films (Fig. 4) of **6a-c** vacuum deposited on OTS treated SiO_2/Si wafers were studied by AFM. For **6b** and **6c**, when the substrate was at 25°C, the

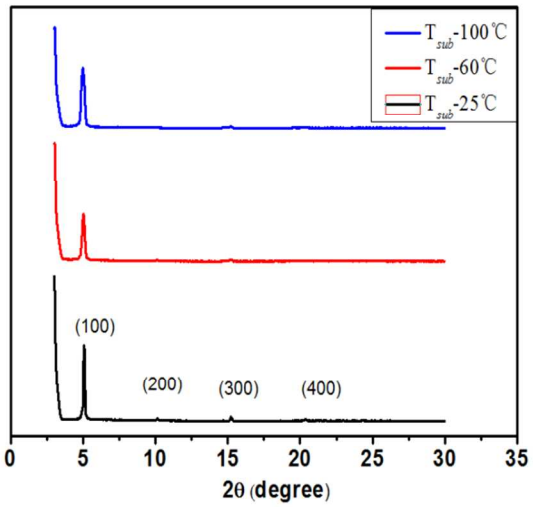

Fig. 5 X-ray Powder diffraction data for **6a**. Here 2θ = 5.06, d-spacing= 1.74nm. Molecular length along its long axis: 2.3nm. Thus the molecules stand on the substrate with a tilt angle of 49°.

Table 1 Detailed performance of OFETs based on **6a-c** thin films.

Compound	T_s/ °C	μ_{max}[a] / $cm^2 V^{-1} s^{-1}$	I_{on}/I_{off}	V_T /V
6a	25	0.07 (0.046)	1 x 10^6	-10
	60	0.30 (0.27)	4 x 10^5	-12
	100	0.32 (0.30)	6×10^4	-14
6b	25	0.0014 (0.0010)	3×10^4	3
	60	0.00008	1×10^4	6
	100	No OFET	-	-
6c	25	0.01(0.0087)	9×10^2	-5.8
	60	0.0044 (0.0034)	6×10^4	14.3
	100	0.00015 (0.0001)	3×10^3	13.8

[a]average values in parentheses

small grains of the film turned larger upon increasing the temperature to 60°C. At 100°C, the films cracked and consequently, film discontinuity and gaps increased. No obvious diffraction peaks could be observed in XRD patterns of the films of **6b**,**c**, indicating the amorphous character of the thin films. For thin films of **6a**, the morphologies changed from the small grains into large continuous area with some particles imbedded in it when the substrate temperature was from r.t to 60°C/100°C. The films of **6a** displayed a series of intense XRD peaks (Fig. 5) belonging to the family of (*h*00), indicating the formation of highly ordered, layered structure. Comparing the *d*-spacing (1.74 nm) with the molecular length (2.30 nm) of **6a** along its long axis, the molecules are expected standing on the substrate with a tilt angle of 49°.

The performance of the OFETs based on **6a-c** is summarized in Table 1. **6a** (100°C) exhibited highest OFET performance among the molecules studied. An average μ_{hole} = 0.32 $cm^2V^{-1}s^{-1}$ with an *on/off* ratio of 1×10^6 (25°C) and a favourable V_T of -10 V was recorded.

The OFET transfer and output characteristics of **6a-c** are shown in Fig. S73, ESI†. Comparing the field-effect mobilities of TTPs **1** reveals that upon substituting phenyl groups at the 5- and 16- positions of **1** (R = H)[14] to obtain **1** (R = Ph)[5] saw a 12.5-fold increase in μ (**1**, R = H: μ = 0.02 $cm^2V^{-1}s^{-1}$, **1**, R = Ph: μ = 0.25 $cm^2V^{-1}s^{-1}$). This could be attributed to the observed change in crystal packing from sandwich-herringbone in the former to face-to-face pattern in the latter, resulting in effective π-π interactions. Upon further substituting the *meso*-aryl substituents of **1** (R = Ph) to create *meso*-*p*-tolyl **1** (R = *p*-MeC_6H_4-),[5] *meso*-*p*-chlorophenyl **1** (R = *p*-ClC_6H_4-)[5] or *meso*-*m*-chlorophenyl **1** (R = *m*-ClC_6H_4-),[10] a decreasing trend of the average hole-mobilities: μ = 0.44, 0.0245 and 0.2 $cm^2V^{-1}s^{-1}$, respectively in that order was recorded. Incidentally, the crystal packing of these compounds adopted a face-to-face pattern. It is clear upon comparing this data and the data recorded in Table 1, that upon changing the *meso*-substituents from H,[14] to Ph,[5] *p*-tolyl,[5] *p*-ethylphenyl **6a**, in that order the field-effect mobility increases, whereas, upon further branching of the alkyl chain (**6b** and **6c**), the hole mobility and hence the device

performance decreases. Further, it has been found that among these compounds, wherever the molecules packed in an asymmetric unit consisting of two molecules, **1** (R = *p*-ClC_6H_4, H)[9,14] and **6b** (R = *p*-^{i}Pr-C_6H_4), the field-effect mobility decreased considerably, while the ones depicting a face-to-face pattern and with adequate chain length showed overall superior hole mobility. The compound **6a** possesses favourable steric and electronic factors and in comparison to **6b** and **6c** yielded crystalline thin films leading to the highest hole mobility of the three. Also, **6a** depicted the highest ambient *on/off* ratio of all the TTPs studied. This is attributed to the direct favourable face to face stacking pattern present in **6a** and also due to the crystalline nature of its thin films thus making it the best tuned molecule for high performance.

Experimental

Materials and methods

^{1}H (400 MHz), ^{13}C (100 MHz) NMR spectra were recorded on a BRUKER AVANCE II 400 NMR Spectrometer and JEOL-FT NMR-AL Spectrometer at 300 MHz, using $CDCl_3$ as the solvent and tetramethylsilane (TMS) as the internal standard. The NMR spectra of final compounds were recorded on a BRUKER 600 AVANCE (III) NMR Spectrometer. The following abbreviations were used to express the multiplicities: s = singlet; d = doublet; t = triplet; q = quartet; m = multiplet; br = broad. Data are reported as follows: chemical shifts in ppm (δ), integration, multiplicity and coupling constant J (Hz). ESI-MS spectra were recorded on Bruker Daltonics esquire 3000_00037 mass spectrometer and an UPLC-Q-TOF instrument, having SYNAPT mass spectrometer and ACQUITY high performance liquid chromatography (WATERS) with a TDA detector. Elemental analyses were performed with a Thermoelectron FLASH EA1112 CHNS analyzer and were within ±0.4% of the theoretical values. FT-IR spectra were recorded on VARIAN 660-IR Fourier-Transform Spectrophotometer and a Perkin Elmer FT-IR spectrometer (Spectrum Two, Serial No:88689) in range 400-4000 cm^{-1} using KBr as a medium. UV-Vis spectra were recorded on a SHIMADZU 1601 PC spectrophotometer, with a quartz cuvette (path length, 1 cm) and studies were performed in AR grade DCM. TGA were performed on a SHIMADZU TGA model DTG-60H. Samples were heated from 50 ^{o}C to 500 ^{o}C with a temp. rise of 10 ^{o}C/minute under nitrogen atmosphere. Electrochemical studies were carried out on CHI 660C Electrochemical Workstation with a conventional three-electrode configuration consisting of platinum working electrode (2 mm diameter), counter electrode and Ag/AgCl as reference electrode. The experiments were carried out on 10^{-4} M solutions of samples in DCM containing 0.1 M tetrabutylammonium hexafluorophosphate ($TBAPF_6$) as supporting electrolyte at room temperature. Deoxygenation of the solutions was achieved by bubbling nitrogen for 30 min and the working electrode was cleaned after each run. The cyclic voltammograms were recorded with a scan rate of 100 mVs^{-1}. All reactions were monitored by thin-layer chromatography carried out on Merck pre-coated TLC plates (silica gel 60 F_{254}, 0.25 mm), visualization by using UV (254 nm). Melting points were determined in open capillaries and are uncorrected. Reactions that required anhydrous conditions were carried out under the blanket of deoxygenated (BASF catalyst) anhydrous nitrogen gas in oven/flame dried glassware. The products were purified by flash column chromatography on silica gel 60-120 mesh. All reagents and chemicals were purchased from Sigma-Aldrich. DMF, Diethyl ether, $TiCl_4$, Pyridine and DCM were purchased locally, dried and distilled prior to use. n-BuLi was prepared and stored under a blanket of dry nitrogen gas. THF and toluene were distilled from sodium/benzophenone (benzophenone ketyl). Anhydrous DCM was stored over fused $CaCl_2$ and distilled before use. Zinc dust was activated prior to use using standard (2M HCl and subsequent water washing) methods. DDQ and hydrazine hydrate were purchased from Sigma-Aldrich, and were used as received. All theoretical studies were performed with a GAUSSIAN 09 software package (Page S50, ESI†).

Device fabrication and characterization

OFET devices were fabricated in the top-contact device configuration. The substrate was heavily doped, n-type Si gate electrode with a 300 nm thick SiO_2 layer as the gate dielectric. The gate dielectric was treated with octadecyltrichlorosilane (OTS) by vapor deposition method. Subsequently, organic semiconductors were deposited on the substrate by thermal evaporation under a pressure of 8×10^{-4} Pa at a deposition rate gradually increased from 0.1 Å s^{-1} to 0.3 Å s^{-1} upto the first 20 nm and then maintained 0.3 Å s^{-1} until the thickness of the film was 50 nm. The deposition rate and film thickness were monitored by a quartz crystal microbalance (ULVAC CRTM-6000). Finally, 20 nm thick gold source and drain electrode were deposited through a shadow mask. The channel length (L) and width (W) were 25 μm and 200μm, respectively. The FET characteristics were measured at room temperature in air using Keithley 4200 SCS. Atomic force microscopy (AFM) measurements were carried out with a Nanoscope IIIa instrument (Digital Instruments) operating in tapping mode. UV-Vis spectra were recorded on a JASCO V-570 spectrometer. The mobilities (μ) were calculated in the saturation regime following the equation: $I_D=\mu C_i(W/2L)(V_G-V_T)^2$, where I_D is the drain current, μ is the field-effect mobility, C_i is the gate dielectric capacitance, W and L are the channel width and length, respectively, V_T is the threshold voltage. X-ray diffraction (XRD) measurements were carried out in the reflection mode at RT using a 2-KW Rigaku X-ray diffractometer (Cu Kα radiation, λ= 1.54Å).

Synthesis

Scheme 1 illustrates the synthesis route of the target compounds.

Synthesis of compound 3

To the mixture of an appropriate aldehyde (100 mmol) and thiophene (300 mmol) was added amberlyst 15 (2.0 g). The mixture was stirred for 3 h at 80 ^{o}C. The mixture was then brought to room temperature and dichloromethane (500 ml) was added to it. The solid was filtered. The solvent was removed by vacuum distillation and the residue was purified by column chromatograph (petroleum ether as eluent) to give compound **3**.

***p*-Ethylphenyl-di(thien-2yl)methane, 3a**

^{1}H NMR (400 MHz, $CDCl_3$): δ (ppm) 7.19 (2H, d, J = 6.36 Hz), 7.09-7.11 (4H, m), 6.85-6.87 (2H, m), 6.77-6.79 (2H, m), 5.79 (1H, s) , 2.59 (2H, q, J = 7.6 Hz), 1.19 (3H, t, J = 7.64 Hz); ^{13}C

NMR (100 MHz, $CDCl_3$): δ (ppm) 147.9, 142.9, 140.9, 128.2, 127.9, 126.5, 125.9, 124.5, 47.1, 28.4, 15.4; IR (KBr): 696, 840, 856, 1036, 1229, 1434, 1511, 2929, 2963, 3021 cm^{-1}; *m/z* 284.9 (M^++1), White solid (Yield = 16%), m.pt. 33-35 °C.

***p*-Isopropylphenyl-di(thien-2yl)methane, 3b**
^{1}H NMR (400 MHz, $CDCl_3$): δ (ppm) 7.19 (2H, d, J = 6.36 Hz), 7.11-7.13 (2H, dd, J = 1.84, 1.72 Hz), 7.07-7.09 (2H, dd, J = 1.2, 1.2 Hz), 6.83-6.85 (2H, m), 6.76-6.78 (2H, m), 5.79 (1H, s), 2.84 (1H, septet, J = 6.88 Hz), 1.20 (6H, d, J = 6.96 Hz); ^{13}C NMR (100 MHz, $CDCl_3$): δ (ppm) 147.86, 147.49, 140.99, 128.18, 126.86, 126.49, 125.88, 124.49, 47.08, 33.64, 23.99; IR (KBr): 545, 696, 840, 857, 1230, 1274, 1362, 1434, 1511, 2959, 3021 cm^{-1}; *m/z* 298.9 (M^++1), colourless oil (Yield = 16%).

***p-tert*-Butylphenyl-di(thien-2yl)methane, 3c**
^{1}H NMR (400 MHz, $CDCl_3$): δ (ppm) 7.27-7.30 (2H, m), 7.19-7.21 (2H, dd, J = 1.8, 1.6 Hz), 7.07-7.08 (2H, dd, J = 1.2, 1.16 Hz), 6.82-6.84 (2H, m), 6.76-6.77 (2H, m), 1.27 (9H, s); ^{13}C NMR (100 MHz, $CDCl_3$): δ (ppm) 149.78, 147.87, 140.63, 127.95, 126.52, 125.93, 125.38, 124.53, 47.02, 34.44, 31.43; IR (KBr): 554, 697, 845, 856, 1230, 1269, 1363, 1514, 2962, 3026 cm^{-1}; *m/z* 313 (M^++1), colourless oil (Yield = 15%).

Synthesis of compound 4
To a solution of *meso-p*-ethylphenyl dithienyl methane (**3a**) 1.036 g (3.65 mmol) in dry diethyl ether (33 ml) was added dropwise, *n*-Buli (8.2 mmol, 2.2 N in hexanes) at r.t.. To the deep red solution so obtained was added dropwise, anhydrous DMF (8 mmol) in diethyl ether. After 1 hour stiring, the mixture was washed sucessively with water, dil. HCl, water and sodium bicarbonate. The organic phase was then dried and vaccum evaporated. The residue was chromatographed on silica to give **4a** as a deep red oil (0.8 g), 62.5%.

***p*-Ethylphenyl-di(5-formylthien-2yl)methane, 4a**
^{1}H NMR (400 MHz, $CDCl_3$): δ (ppm) 9.83 (2H, s), 7.64 (2H, d, J = 3.8 Hz), 7.19 (4H, s), 6.97-6.98 (2H, m), 5.86 (1H, s), 2.64 (2H, q, J = 7.6 Hz), 1.23 (3H, t, J = 7.6 Hz); ^{13}C NMR (100 MHz, $CDCl_3$): δ (ppm) 182.87, 157.14, 144.36, 143.16, 138.32, 136.40, 128.57, 128.18, 127.68, 48.33, 28.48, 15.42; IR (KBr): 670, 760, 814, 1046, 1221, 1450, 1512, 1526, 1665, 2748, 2807, 2965, 3023, 3088 cm^{-1}; *m/z* 341 (M^++1), Redish brown viscous liquid (Yield = 62.5%).

***p*-Isopropylphenyl-di(5-formylthien-2yl)methane, 4b**
^{1}H NMR (400 MHz, $CDCl_3$): δ (ppm) 9.72 (2H, s), 7.54 (2H, d, J = 3.6 Hz), 7.09 (4H, s), 6.88-6.92 (2H, m), 5.77 (1H, s), 2.80 (1H, septet, J = 6.90 Hz), 1.14 (6H, d, J = 6.90 Hz); ^{13}C NMR (100 MHz, $CDCl_3$): δ (ppm) 182.90, 157.17, 148.94, 143.14, 138.36, 136.42, 128.15, 127.68, 127.14, 48.32, 33.76, 23.93; IR (KBr): 672, 772, 817, 1045, 1217, 1445, 1523, 1657, 2803, 2848, 2920, 2959 cm^{-1}; *m/z* 355 (M^++1), Light brown solid (Yield = 62.3%), m.pt. 56-58 °C.

***p-tert*-Butylphenyl-di(5-formylthien-2yl)methane, 4c**
^{1}H NMR (400 MHz, $CDCl_3$): δ (ppm) 9.83 (2H, s), 7.63-7.64 (2H, d, J = 3.84 Hz), 7.36-7.38 (2H, dd, J = 1.88, 1.96 Hz), 7.20-7.22 (2H, dd, J = 1.76, 1.72 Hz), 6.98-6.99 (2H, dd, J = 0.76, 0.60 Hz), 5.87 (1H, s), 1.31 (9H, s); ^{13}C NMR (100 MHz, $CDCl_3$): δ (ppm) 182.89, 157.15, 151.21, 143.15, 137.99, 136.42, 127.88, 127.70, 126.00, 48.24, 34.61, 31.31; IR (KBr): 672, 772, 822, 1045, 1117, 1217, 1445, 1523, 1662, 2809, 2864, 2953, 3037, 3293 cm^{-1}; *m/z* 369 (M^++1), Light brown solid (Yield = 60%), m.pt. 103-105 °C.

Synthesis of compound 5

To a stirring suspension of zinc dust (38 mmol) in 200 ml of THF maintained under nitrogen atmosphere, a solution of 19.6 ml of 1.0 M $TiCl_4$ (in CH_2Cl_2) was added over 20 minutes. The reaction mixture was refluxed for 1 hour, and treated with a solution of appropriate dialdehyde (1.78 mmol) and pyridine (35.6 mmol) dissolved in 200 ml of THF. The addition was made using a hypodermic syringe over 40 minutes to the gently refluxing suspension. After refluxing under nitrogen for 18 hours, the reaction was carefully quenched with a solution of aqueous K_2CO_3 (10%, 100 ml). The reaction mixture was filtered through a celite bed, and the filtrate was concentrated under reduced pressure and the residue extracted with 300 ml methylene chloride. The extract was washed with water (2 x 50 ml) and dried over anhydrous sodium sulfate. The solvent was evaporated under reduced pressure and the residue was chromatographed (over silica) to isolate the **5a-c** as light green solids (15%), (**5a-c**, m.pt. >280 ^{o}C).

***Meso-p*-Ethylphenyldihydrotetrathia[20]porphyrin[2.1.2.1], 5a**
^{1}H NMR (400 MHz, $CDCl_3$): δ (ppm) 7.22-7.25 (4H, m), 7.14-7.16 (4H, m), 6.80 (4H, t, J = 3.44 Hz), 6.61-6.65 (4H, m), 6.48 (4H, d, J = 3.4 Hz), 5.71-5.73 (2 H, m), 2.63 (4H, q, J = 5.28 Hz), 1.22 (6H, t, J = 5.6 Hz); ^{13}C NMR (100 MHz, $CDCl_3$): δ (ppm) 149.4, 143, 140, 138.4, 128.4, 127.9, 125.4, 123.4, 48, 47.8, 29.6, 28.4, 15.4; IR (KBr): 794, 817, 1017, 1100, 1228, 1395, 1451, 1507, 1607, 1907, 2302, 2864, 2926, 2959, 3015 cm^{-1}; *m/z* 617.1341 (M^++1), Greenish solid (Yield = 14%), m.pt. >250 °C.

***Meso-p*-Isopropylphenyldihydrotetrathia[20]porphyrin[2.1.2.1], 5b**
^{1}H NMR (400 MHz, $CDCl_3$): δ (ppm) 7.23-7.25 (4H, m), 7.16-7.21 (4H, m), 6.80 (4H, t, J = 3.28 Hz), 6.61-6.65 (4H, m), 6.48 (4H, d, J = 3.44 Hz), 5.71-5.73 (2H, m), 2.89 (2H, septet, J = 4.84 Hz), 1.23 (12H, d, J = 3.2 Hz); ^{13}C NMR (100 MHz, $CDCl_3$): δ (ppm) 149.4, 147.6, 140.1, 140, 138.5, 138.4, 128.3, 126.5, 125.4, 123.4, 48, 47.9, 33.6, 29.6, 23.9; IR (KBr): 811, 1017, 1095, 1262, 1418, 1457, 1507, 1590, 1674, 1907, 2297, 2859, 2926, 2953, 3015, 3054 cm^{-1}; *m/z* 645.1650 (M^++1), Greenish solid (Yield =15%), m.pt. >250 °C.

***Meso-p-tert*-Butylphenyldihydrotetrathia[20]porphyrin[2.1.2.1], 5c**
^{1}H NMR (400 MHz, $CDCl_3$): δ (ppm) 7.32-7.35 (4H, m), 7.24-7.26 (4H, m), 6.80 (4H, t, J = 3.28 Hz), 6.61-6.65 (4H, m), 6.49 (4H, d, J = 3.48 Hz), 5.71-5.73 (2H, m), 1.30 (18H, s); ^{13}C NMR (100 MHz, $CDCl_3$): δ (ppm) 149.8, 149.4, 149.3, 139.7, 138.5, 138.4, 128.3, 128, 125.5, 125.4, 123.4, 48, 47.8, 34.4, 31.3, 29.6; IR (KBr): 783, 817, 1017, 1106, 1201, 1267, 1362, 1390, 1462, 1507, 1607, 1735, 2853, 2926, 2953, 3015, 3065 cm^{-1}; *m/z* 673.1939 (M^++1), Greenish solid (Yield =15%), m.pt. >250 °C.

Synthesis of compound 6

To a solution of **5a** (0.2 mmol) in 5 ml toluene, was added under nitrogen with stirring, a solution of DDQ (0.6 mmol) in 5 ml toluene. Shortly after mixing the two solutions, purple

precipitates formed and the reaction mixture was stirred for additional 3 h. The purple precipitates were filtered and added to 5 ml of hydrazine hydrate (98%). After boiling for 10 minutes, the solid was filtered, washed with water, and dried. The resulting product was dissolved in methylene chloride and chromatographed on silica (DCM). Evaporation of the purple solution gave **6a** (50%) as shining metallic purple solid (**6a-c**, m.pt. >280 ^{o}C).

***Meso-p*-Ethylphenyltetrathia[22]porphyrin[2.1.2.1], 6a**
^{1}H NMR (600 MHz, $CDCl_3$): δ (ppm) 11.02 (4H, s), 10.34 (4H, d, J = 4.5 Hz), 10.01 (4H, d, J = 4.2 Hz), 8.37 (4H, d, J = 7.68 Hz), 7.81 (4H, d, J = 7.62 Hz), 3.15 (4H, q, J = 7.8 Hz), 1.66 (6H, t, J = 7.8 Hz); ^{13}C NMR (150 MHz, $CDCl_3$): δ (ppm) 137.90, 136.89, 133.98, 130.38, 127.57, 113.51, 31.89, 29.35, 24.85, 22.62, 15.73, 14.00; IR (KBr): 811, 1017, 1117, 1167, 1340, 1445, 1507, 1590, 2302, 2864, 2926, 2965, 3271 cm^{-1}; Anal. Calcd. (%) for $C_{38}H_{30}S_4$: C, 74.26; H, 4.88; S, 20.84; Found: C, 74.28; H, 4.88; S, 20.84; *m/z* 615.1178 (M^++1), Purple solid (Yield = 50%), m.pt. >250 °C.

***Meso-p*-Isopropylphenyltetrathia[22]porphyrin[2.1.2.1], 6b**
^{1}H NMR (600 MHz, $CDCl_3$): δ (ppm) 11.04 (4H, s), 10.36 (4H, d, J = 4.5 Hz), 10.02 (4H, d, J = 4.26 Hz), 8.39 (4H, d, J = 7.74 Hz), 7.85 (4H, d, J = 7.68 Hz), 3.40-3.43 (2H, m), 1.69 (12H, d, J = 6.6 Hz); ^{13}C NMR (150 MHz, $CDCl_3$): δ (ppm) 148.85, 136.88, 133.39, 130.41, 126.13, 113.49, 34.34, 34.05, 29.65, 24.34, 22.62, 14.00; IR (KBr): 811, 1017, 1162, 1184, 1334, 1356, 1406, 1457, 1501, 1796, 1907, 2864, 2953, 3020, 3054 cm^{-1}; Anal. Calcd. (%) for $C_{40}H_{34}S_4$: C, 74.76; H, 5.29; S, 19.93; Found: C, 74.75; H, 5.29; S, 19.92; *m/z* 643.1478 (M^++1), Purple solid (Yield = 50%), m.pt. >250 °C.

***Meso-p-tert*-Butylphenyltetrathia[22]porphyrin[2.1.2.1], 6c**
^{1}H NMR (600 MHz, $CDCl_3$): δ (ppm) 10.99 (4H, s), 10.31 (4H, s), 9.98 (4H, s), 8.36 (4H, s), 7.96 (4H, s), 1.70 (18H, s); IR (KBr): 811, 1017, 1123, 1189, 1262, 1362, 1390, 1457, 1590, 2347, 2948, 3349 cm^{-1}; Anal. Calcd. (%) for $C_{42}H_{38}S_4$: C, 75.22; H, 5.67; S, 19.10; Found: C, 75.24; H, 5.66; S, 19.10; *m/z* 671.1789 (M^++1), Purple solid (Yield = 45%), m.pt. >250 °C.

Conclusions

In summary, a facile, high yielding synthesis of new *meso*-substituted TTPs is described. Compared to the previously reported TTPs, these materials depicted much improved *on/off* ratios. μ_{hole} is much superior to analogous α-oligothiophenes. This difference, highlight the role that neutral 5,16-disubstituted TTPs can play in the development of potentially useful OFETs. Further, no inert conditions were required and both the molecules and devices were stable in air. Chemical substitution is thus a powerful molecular design tool to tune the packing motifs of these organic semiconductors, their solubilities and their corresponding electronic properties.

Acknowledgements

KS thanks DST, New Delhi for financial assistance (SB/S1/OC-45/2013). TSV thanks CSIR, New Delhi, for a Senior Research fellowship (letter no. 09/254(0246)/2012-EMR-I). Thanks are due to SIC, IIT Indore for X-ray analysis and IISER (Mohali) for recording TGA and SAIF, PU, Chandigarh for recording NMR spectra.

Notes and references

1 H. Wang, C. S. Hamann, F. Marchioni and F. Wudl, *Adv. Mater.*, 2007, **19**, 558-560.
2 C. Wang, H. Dong, W. Hu, Y. Liu and D. Zhu, *Chem. Rev.*, 2012, **112**, 2208–2267.
3 O. Gidron, A. Dadvand, Y. Sheynin, M. Bendikov and D. F. Perepichka, *Chem. Commun.*, 2011, **47**, 1976–1978.
4 Y. Song, C.-a. Di, X. Yang, S. Li, W. Xu, Y. Liu, L. Yang, Z. Shuai, D. Zhang and D. Zhu, *J. Am. Chem. Soc.*, 2006, **128**, 15940-15941.
5 K. Singh, A. Sharma, J. Zhang, W. Xu and D. Zhu, *Chem. Commun.*, 2011, **47**, 905–907.
6 K. Singh, T. S. Virk, J. Zhang, W. Xu and D. Zhu, *Chem. Commun.*, 2012, **48**, 121–123.
7 J. Zhang, H. Geng, T. S. Virk, Y. Zhao, J. Tan, C.-a. Di, W. Xu, K. Singh, W. Hu, Z. Shuai, Y. Liu and D. Zhu, *Adv. Mater.*, 2012, **24**, 2603-2607.
8 J. Zhang, J. Tan, Z. Ma, W. Xu, G. Zhao, H. Geng, C.-a. Di, W. Hu, Z. Shuai, K. Singh and D. Zhu, *J. Am. Chem. Soc.*, 2013, **135** (2), 558–561.
9 J. Zhang, Z. Ma, Q. Zhang, T. S. Virk, H. Geng, D. Wang, W. Xu, Z. Shuai, K. Singh, W. Hu and D. Zhu, *J. Mater. Chem. C*, 2013, **1**, 5765-5771.
10 K. Singh, T. S. Virk, J. Zhang, W. Xu and D. Zhu, *Chem. Commun.*, 2012, **48**, 12174-12176.
11 D. S. Garcia and J. L. Sessler, *Chem. Soc. Rev.*, 2008, **37**, 215–232.
12 A. Stanger, *J. Org. Chem.*, 2006, **71**, 883-893.
13 Z. Hu, J. L. Atwood and M. P. Cava, *J. Org. Chem.,* 1994, **59**, 8071-8075.
14 T. Zhao, Z. Wei, Y. Song, W. Xu, W. Hu and D. Zhu, *J. Mater. Chem.*, 2007, **17**, 4377-4381.